

Article

New Empirical Path Loss Model for 28 GHz and 38 GHz Millimeter Wave in Indoor Urban under Various Conditions

Zyad Nossire ^{1,*}, Navarun Gupta ¹, Laiali Almazaydeh ² and Xingguo Xiong ^{1,*}¹ University of Bridgeport, Bridgeport, CT 06604, USA; navarung@bridgeport.edu² Al Hussein Bin Talal University, 71110 Ma'an, Jordan; Laiali.almazaydeh@ahu.edu.jo

* Correspondence: znossire@my.bridgeport.edu (Z.N.); xxiong@bridgeport.edu (X.X.);

Tel.: +1-203-953-6425

Received: 26 September 2018; Accepted: 25 October 2018; Published: 1 November 2018



Abstract: Due to rapid development in mobile communication technology in recent years, the demand for high quality and high capacity networks with thorough coverage has become a major necessity. Several models have been developed for predicting wireless signal coverage in urban areas, but these models suffer from inadequately calculating certain conditions, such as weather and building materials, especially window size. In this paper, we propose a new path loss prediction model based on the measurement of new indicators, such as window size, temperature, and humidity conditions, after which an extensive statistical analysis using a linear regression technique was implemented in order to validate the new indicators. As the new indicators were incorporated into the Okumura model to derive a new path loss model, the results showed that the proposed model provides an accurate prediction of the received signal strength in a given propagation environment. Our model enhanced the prediction of path loss by 10% when compared to the Okumura and by 15% when compared to the COST-Hata.

Keywords: path loss; signal; millimeter wave; Okumara; COST-Hata; window size; temperature; humidity

1. Introduction

The increasing demand for mobile data in daily life, as well as the importance of high-speed data transmission, has led to enormous growth of mobile communication systems. To a large extent, mobile communication systems have witnessed major advances in wireless access, integrated circuits, and digital signal processing, which have brought about additional technologies such as Global positioning system (GPS), IP telephony, online gaming, streamed multimedia, and ultra-broadband internet access [1].

There are two primary limitations to the performances of the 4G mobile communication systems: time and location. The new 5G technology, with 28 and 38 GHz mm wave frequencies, address these limitations [2]. Amongst the channel characteristics, signal paths change is the most critical parameter. The path loss is defined as a decrease in the signal strength during propagation from the transmitter to the receiver [3]. Several effects may cause the path loss, such as reflection, refraction, diffraction, absorption, coupling, and cable loss [4]. The path loss inside the building is also influenced by many factors, including the propagation medium, environment, height of the antennas, and the distance between the transmitter and the receiver inside the building [5,6]. Figure 1 shows the effect of path loss on the received signal power over an urban area and inside building obstacles. However, there is a clear relationship between the signal strength and the temperature. In general, when the temperature increases, the Received Signal Strength Indicator (RSSI) drops [7]. Naturally, the relative humidity

increases and drops based on RSSI, which is dependent on a positive relationship with the trend of Absolute Humidity (AH), indicating a negative correlation [8]. If the size of a window is large the signal will be high; if the window size decreases, the signal will decrease [9,10].

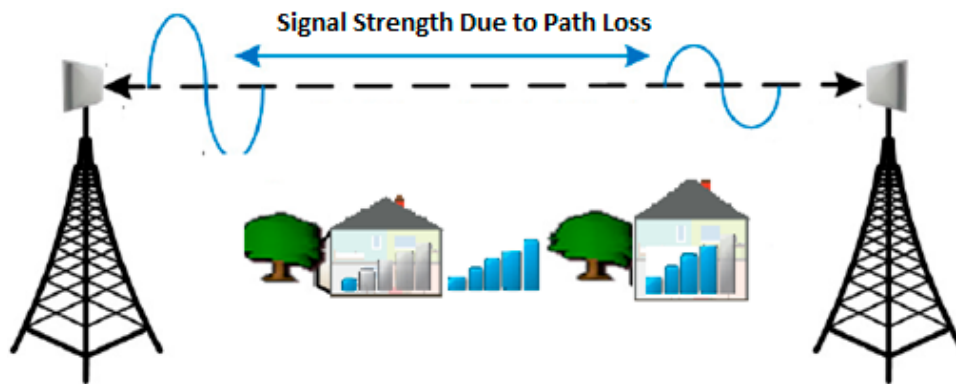


Figure 1. Different path loss sensor (signal strength).

Radio channels are random. In order to predict path loss, the radio channels must be modeled [4]. Therefore, for practical path loss prediction, propagation models are used. Among these models are the Okumura, COST-Hata, and empirical models, which are all used extensively. Path loss calculation is typically done based on observations and data measurements, such as the distance of the receiver from the transmitter and signal frequency. These two measures are manipulated in a logarithmic format as given in Equation (1).

$$PL = 32.45 + 20 \log_{10}(d) + \log_{10}(f) \quad (1)$$

Definition 1. (PL) is the path loss, (d) is the distance between the sender (TX) and the receiver (RX), and (f) is the frequency, the (32.45) is the coefficient. This model is the basic model for all path loss models.

Among the most broadly used empirical models are the Okumura model and COST-Hata model [4]. Okumura model is applicable in the frequency range 3 GHz [3,5], whereas COST-Hata model gives simple and straightforward techniques to ascertain path loss in a wider frequency range. Despite the fact that working frequency (5 GHz) is well beyond its estimation extent, its effortlessness and adjustment variables still allow for the calculation of path loss occurring at higher frequencies. The Okumura and COST-Hata models are an accepted standard of today's propagation prediction models, but both models do not consider certain pertinent effects, such as indoor and outdoor environments, humidity, temperature, and window size. This paper proposes a path loss propagation model that illuminates new indicators like windows size and weather conditions. Thus, our findings help telecommunication providers in network planning to design stable mobile indoor networks that work accurately with the high and low power signal.

The remainder of this paper is structured as follows: Section 2 presents related work for path loss models; Section 3 presents details on the analysis methodology of the proposed model; Section 4 demonstrates the evaluation and results of the proposed model Section 5 concludes this paper by considering the potential usefulness of the model system.

2. Related Works

Over the past few years, several low frequency models have been developed for path loss prediction [11]. Concerning the related models, the Okumura model [4] is the classical empirical model, while most of the other models are derived from Okumura's model.

Moreover, the wireless industry is moving to its fifth generation of cellular technology. This technology will bring mobility to millimeter waves (mmWave) communications. Fifth generation cellular networks (5G) offer unprecedented bandwidth and faster network speeds by tapping into a high band spectrum in the mmWave frequency range, typically from 30 to 300 GHz [12,13]. Propagation is more lossy in the mmWave bands when compared to today’s microwave bands, thus the solution is to modify the standard path loss models (with a frequency between 28 and 38 GHz) to fit the real world measured propagation data for reliable mmWave channel planning [14,15]. However, the previous models (Okumura, COST-Hata) do not work with frequencies between 28 and 38 GHz, and thus they are not compatible with the 5G [16,17].

Of all the literature studies, the Okumura model [18] is the foundation of today’s propagation prediction models. This prediction model is based on data extensive measurements which enable the telecommunication providers to compute the received signal power in a given propagation medium. However, when making network planning in practice, it is required to fit the parameters that was best used in the Okumura model, instead of a direct usage. In this regard, an empirical formulation for propagation prediction called a COST-HATA model [19] is derived from Okumura’s model. This model offers straightforward techniques to verify path loss in an expandable frequency range. On the other hand, our working frequency of 5 GHz is different from the estimation extent, as its effortlessness and modified variables still allow us to estimate the path loss at a higher frequency.

Furthermore, it provides a good approximation in urban areas and it is a well-suited model over roughly the same range of Okumura converge frequencies, as the model for urban areas was built first and used as the base for other models. By using the Okumura model, we have the ability to calculate path loss in urban areas up to less than 3 GHz [20].

The path loss model by Okumura is given according to Equation (2).

$$PL = lf + A_{mu}(f, d) - G_{(hte)} - G_{(hre)} - G_{area} \tag{2}$$

Definition 2.

PL: is Path loss.

lf: is the free space propagation loss.

A_{mu}(f, d): is the median attenuation relative to free space.

G_(hte): is the gain base station antenna.

G_(hre): is the gain mobile antenna.

G_{area}: is the gain due to the type of environment.

The COST-Hata models have more parameters that allow frequency and height to be adjusted. The Okumura and COST-Hata models are more generalized and well-known.

The Hata path loss model is represented in Equation (3).

$$PL = 46.3 + 33.9 \log_{10}(f) - 13.82 \log_{10} - ahm + (44.9 - 6.55 \log_{10}(hb)) \log_{10}(d) + cm \tag{3}$$

Definition 3. *d* is for distance, *hb* is the height of the transmitter antenna, *ahm* is the Height of mobile station antenna, and *cm* is the height correction factor; *ahm* and *cm* have two values depending on the area being tested, as listed below:

Urban area: ahm = 3.2(log₁₀ 11.75)) 2 - 4.79.

Urban area: cm = 3 dB.

The classical Okumura and COST-Hata models are also examined [8]. Fuzzy logic was applied as a set of rules to characterize precisely the unknown propagation environment from a set of known

propagation environments. As a result, more cost-effective cellular network designs are expected using the path method.

Other path loss prediction models created by Miura et al. [8] made use of the sum of three propagation losses: propagation loss, wall penetration loss, and indoor propagation loss. That is, the radio waves coverage outdoor to indoor by propagating from the transmitter outdoor to the wall of the building. Then, the radio waves penetrate the wall of the building. Last, the radio waves propagate inside the building to the receiver.

Later, such methods [8,21], aimed at using artificial neural networks (ANNs) model to predict path loss. The ANNs perform a nonlinear mapping function of a given set of input values to a set of appropriate output values. Thus, the input parameters contain propagation features, such as frequency, the distance between the transmitter and the receiver, and the desired output value, which contains the measured path loss for a better prediction.

Other such models are Hata [8], COST 231 HATA [21], Walfisch [9], Stanford University Interim (SUI) [9], and the ECC-33 model [22]. These models have previously been compared [23].

Based on the related models in this field, the Okumura model [24] and the COST 231 HATA model [25,26] are both used as a basis for our proposed model, given that these models cover a wide range of frequencies as well as different terrains with a high accuracy. Other models are limited to significant restrictions, such as the antenna height or covered building height, because most of these models also show low accuracy over some terrains [27–29].

Femtocells have risen as a promising solution in order to address the path loss issue and to decongest the microcell network from the increasing number of mobile users and corresponding traffic. As such, 90% of data services and 60% of phone calls take place within an indoor environment. Femtocells, which usually reside in a home/office environment and consist of an Access Point (AP) with short range (i.e., 10–50 m) are connected to a service provider's Internet network. They can provide large indoor coverage and capacity due to the short communication distance to users. Furthermore, femtocells are characterized by low cost installation over an existing microcell network. In the area of two-tier femtocell networks, the overlapping of the coverage areas of femtocells and microcell offer the ability to connect to either the Microcell or a neighboring femtocell, depending on the quality of service criteria. One of the major challenges in this area is that femtocells share the same licensed frequency with microcells [30–32].

In this paper, the proposed prediction model is based on measurement of new indicators and extensive statistical analysis, in order to compute the predicted received signal strength in a given propagation environment. We present a new path loss model that includes new parameters allowing for an accurate estimation of signal power inside of buildings, as well as the distance between transmitter and receiver. However, the Okumura and COST-Hata models do not take into consideration other factors like the buildings. Therefore, many models were proposed like Okumura, and COAST-Hata. They were the most widely used though our new model was an enhancement over them.

3. Proposed Model

The main focus of this research is to develop a new path loss prediction model, which we will call the TYM model (see Equation (7)). The success of the TYM model depends on new parameters, as it works in one type of environment like urban areas with a frequency ranging from 28 to 38 GHz. The proposed approach is comprised of two main steps: dataset gathering and coefficient calculation using a linear regression technique. The details of these main steps will be explained, in addition to the effects of the new parameters on the proposed model.

3.1. The Effects of the New Parameters on the TYM

Temperature and humidity are significantly related to each other. Humidity is the amount of water steam present in the air and it is ordinarily invisible. The highest level of water steam in the air is based on the changeable temperature of the air. The temperature point implies that the air should

cool down so that the water steam reduces into either ice or water ($RH = 100\%$) [7]. Steam from boiling water changes from a gassy state into a solid (deposition, $T < 0\text{ }^\circ\text{C}$) state or into a liquid (intensification) state. Intensification/deposition begins when the temperature precipitation or the humidity reaches a saturation point of ($RH = 100\%$). The steam from the water is either called clouds (fog) or dew (frost when $T < 0\text{ }^\circ\text{C}$), but this depends on the weather condition [7,8].

$$AH(t, RH) = 216.7 \cdot \left\{ \frac{\frac{RH}{100\%} \cdot A \cdot \exp\left(\frac{m \cdot t}{T_n + t}\right)}{273.15 + t} \right\} \tag{4}$$

Definition 4. (t) denotes the actual temperature ($^\circ\text{C}$), RH denotes the actual relative humidity (%), (m) = 17.62, (T_n) = 243.12 $^\circ\text{C}$, and (A) = 6.112 hPa, (AH) denotes the Absolute Humidity.

3.1.1. Effects of Temperature on Signal Strength

There is a clear relationship between signal strength and temperature. Generally, when the temperature increases, RSSI drops, and vice versa, which represents a negative relationship between signal strength and temperature [8].

3.1.2. The Impact of Humidity on Signal Strength

To measure the different aspects of humidity, we used: Absolute Humidity (AH), which refers to the total mass of steam from water included in a given air volume; Steam Humidity (SH) is the highest amount of steam from water in the air at a given temperature; Relative Humidity (RH) is the amount of AH that exists in the air and thus refers to the highest amount of SH at the same pressure and temperature. The relative humidity of the SH is 100%. Humidity is considered as another variable that puts an impact on the signal strength. It is obvious that the relationship between both AH and RH humidity affects the signal strength within a given time. The relative humidity increases and drops based on RSSI, and this depends on a positive relationship, while the trend of AH, indicates a negative correlation (Table 3) [7].

3.1.3. The Impact of Window Size on Signal Strength

Here, we shall explain some of the features of window size. Specifically, the effect of both the metal frame shape over the deviation style and the window size; both must be taken into consideration, in addition to the view of a computational accuracy spot.

Another important factor that needs to be considered is the effect of window size on the form of the deviation style [9,10]. For the window size, the complete area of the entire window is calculated in this paper within the same selected floor. In fact, this process was performed by conducting calculations for the average size of each entire window. Then, we performed a multiplication for the available number of windows.

In relation to the window size inside the building, we calculated the full surface area for the window in the same specific floor. This was accomplished by multiplying the average size for all the windows in the same floor by the number of the windows (Equation (5)).

$$S_{win} = \frac{1}{N} \sum_{i=1}^N a_i = \frac{1}{N} = (win_1 + win_2 + \dots + win_n) \tag{5}$$

Definition 5. (S_{win}) is window size, (N) is the number of windows, (win_n) is number of windows in each floor.

3.2. Measurements and Environment Definitions for Urban Area

Using the real data measurement, we now suggest that there are several empirical path loss models suitable for the signal mobile system, using the sender (TX) and receiver (RX), for 5G mmWave wireless networks with a frequency between 28 GHz and 38 GHz. The measurement frequency between 28 GHz and 38 GHz came from a broadband sliding channel effect, using (BPSK) identical binary shift keying and modulated Pseudo-noise (PN). The 28 GHz combine 11.2° and 28.9° half-power bandwidth (HPBW) antennas at the sender (TX) and receiver (RX). The 38 GHz combine 9.2° and 49.7° half-power bandwidth (HPBW) antenna at receiver (RX) [14–16]. The measurement propagation [14–16] combines power delay profiles (PDPs) for single point angles using high directions (8, 19).

The data measurement for microwave path loss models was collected in different places in an urban area (Tables 1 and 2). In order to show the non-line-of-sight (NLOS) for the different frequency between 28 GHz and 38 GHz mmWave bands (Table 1), we introduced the empirical path loss model and show the statistics with 10 m free space distance for a range of locations, and the directional RX antennas for each location.

Table 1. Measurements between the sender (TX) and the receiver (RX) with a frequency of 38 GHz.

Environment	NLOS	
TX height antenna (m)	8	19
RX height antenna (m)	1.55	
TX gain antenna (dB)	24.8	
TX(HPBW) (°)	11.2°	
RX gain antenna (dB)	24.8	16
RX (HPBW) (°)	11.2°	28.9°

The tables provided simple mmWave path loss models that are functional with the height and frequency for different directions. The definitions of the environment used in Tables 1 and 2 explained that the RX locations were classified according to the NLOS definition:

NLOS refers to the path of propagation of a radio frequency (RF) that is obscured (partially or completely) by obstacles, thus making it difficult for the radio signal to pass through (Figure 2). Common obstacles between radio transmitters and radio receivers are tall buildings, trees, physical, scape, and high-voltage power conductors. While some obstacles absorb and others reflect the radio signal; similarly, they all limit the transmission ability of signals (Figure 2) [6].

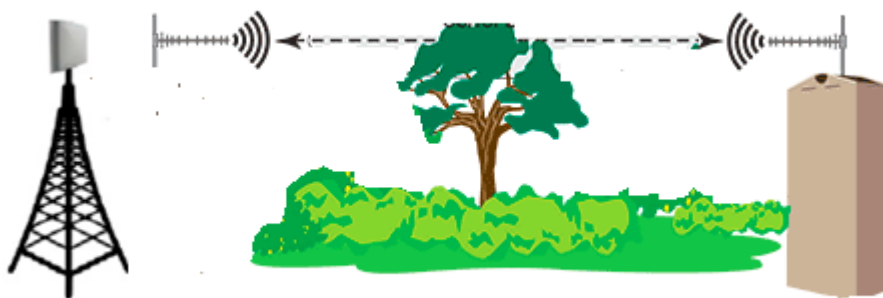


Figure 2. Visual representation of a non-line-of-sight (NLOS).

The signal was measured at 28 GHz RX at the University of Bridgeport, Connecticut, USA (see Figure 3 for different locations). The green dots in Figure 3 show the distances at the TX locations, which went up to 300 m. For RX locations, we used half-power Beam width antennas (HPBW) with 25.3 dB (11.2° HPBW) and 16 dB (28.9° HPBW) gain antennas at the TX and RX for the largest range of measurement of 184 dB incoming signals from different angles of arrivals. The data measurement was collected over distances of 25 to 500 m but was cut from 20 to 251 m based on the power failure [14].

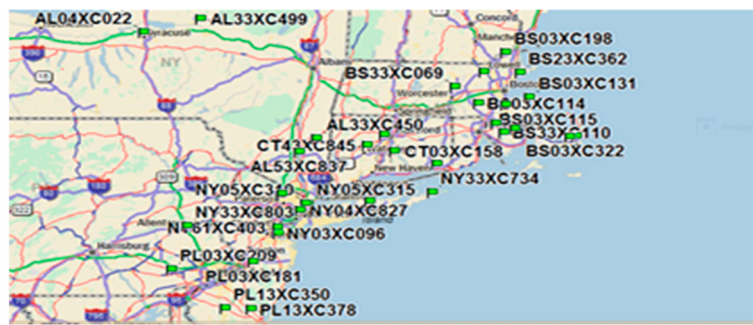


Figure 3. Measurement locations (University of Bridgeport, CT, USA).

For the frequency of 38 GHz propagation (Table 2), the signal was measured at 38 GHz RX at the University of Bridgeport, Connecticut, USA (see Figure 3 for different distances up to 300 m with six different handheld measurements, using two different transition locations). There were six handheld RX locations using half-power Beam width antennas (HPBW). Most TX-RX locations used 25.3 dBi (9.2° HPBW) gain directional antennas, while others used 14 dBi gain (49.7° HPBW) antennas at the RX. The data measurement was collected over distances of 25 to 500 m [14].

Table 2. Measurements between TX and RX with a frequency of 38 GHz.

Environment	NLOS					
TX height antenna (m)	24		9		38	
RX height antenna (m)	1.55					
TX gain antenna (dB)	25.3					
TX (HPBW) (°)	9.2°					
Handheld RX gain antenna (dB)	25.3°	14°	25.3°	14°	25.3°	14°
Handheld RX (HPBW) (°)	9.2°	49.7°	9.2°	49.7°	9.2°	49.7°

Tables 1 and 2 show path loss at a 3 m frequency for a distance signal, which was obtained with a high antenna gain at 28 and 38 GHz. The NLOS measurement data in these tables is closely modeled by the environment parameters for the path loss model. The measured results in Tables 1 and 2 were determined by using a 6 m free space distance between TX and RX and were obtained using a liner regression model ranging between 28 and 38 GHz. The measured results in Tables 1 and 2 were determined by using a 10 m free space distance between TX and RX and were obtained using a liner regression model ranging between 28 and 38 GHz.

3.3. Dataset Gathering

For the dataset reading, we collected data from multiple geographical locations inside and outside of the University of Bridgeport. This measurement was collected to help build the TYM model. The dataset contains between 28 and 38 GHz path loss measurements, collected from 35 base stations. The dataset reading used AT&T company tools from inside buildings, especially inside elevators. Table 3 shows measurements for random samples of the collected dataset.

Table 3. Random measurements from the collected dataset.

Window Size	Temperature	Humidity	Frequency
32.13	82 °F	65%	(28) GHz
27.21	82 °F	65%	(28) GHz
25.49	82 °F	65%	(28) GHz
24.21	82 °F	65%	(28) GHz
27.23	82 °F	65%	(28) GHz
10.14	82 °F	65%	(28) GHz
23.23	82 °F	65%	(28) GHz

3.4. New Parameters Coefficient Calculation Using a Linear Regression Technique on TYM Model

The linear regression technique “is a form of predictive modelling technique which investigates the relationship between a dependent and independent variable. This technique is used for calculating time series modelling and findings between the variables” [28].

$$Y = a + b * X + e \tag{6}$$

Definition 6. *b* is the slope of the line and *e* is the error term. This equation can be used to predict the value of target variable based on given predictor variable.

For fitting a regression line, it calculates the best-fit line for the observed data by minimizing the sum of the squares of the vertical deviations from each data point to the line [28].

3.5. TYM Model

Based on the linear regression technique on the different parameters we have formulated a new model called the TYM model. This model shows that the path loss value is highly dependent on these parameters: distance between the transmitter (TX) and receiver (RX), temperature, humidity, window size, and the frequency. The TYM model is represented in Equation (7).

$$PL = 96.7 - 0.562 * S_{win} - 0.366 * f + 0.092 * d - 0.187 * h + 0.257 * t \tag{7}$$

Definition 7. (*PL*) is path loss, (*S_{win}*): window size, (*f*): Frequency, (*d*): distance between sender and receiver, (*h*): humidity, (*t*): temperature, and the number before every variable and its coefficient.

Based on the linear regression technique on the window size parameter, using a TYM model in Figure 4, shows the regression of the path loss by the window size with coefficients (0.562). If the size of the window is big, the path loss will be low, which means the relation is negative.

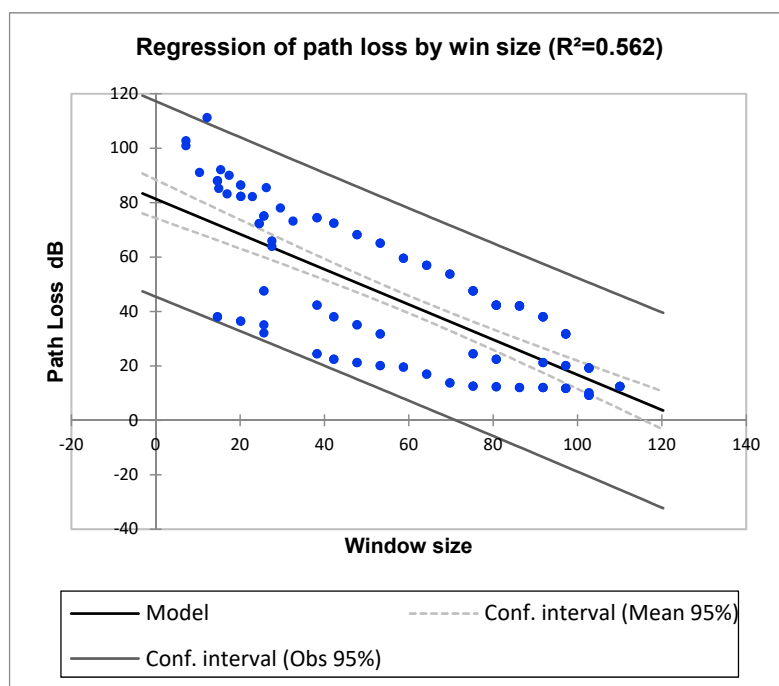


Figure 4. Regression of path loss by the window size.

Based on the linear regression technique on the window size parameter, Figure 5 shows the regression of the path loss between the distance and the receiver with coefficients (0.092). If the distance between the sender and the receiver is very close, the path loss will be low, which means that the relation is positive.

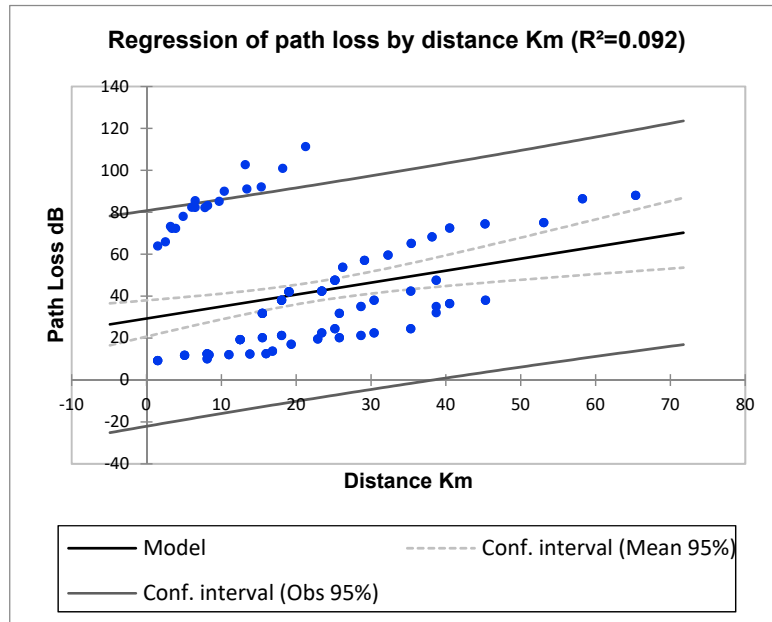


Figure 5. Regression of Path Loss by Distance.

Based on the linear regression technique on the humidity parameter, Figure 6 shows the regression of the path loss by the humidity with coefficients (0.187). The relative humidity increases, and drops based on (RSSI), and is depended on a positive relationship, while the trend of AH indicates a negative correlation.

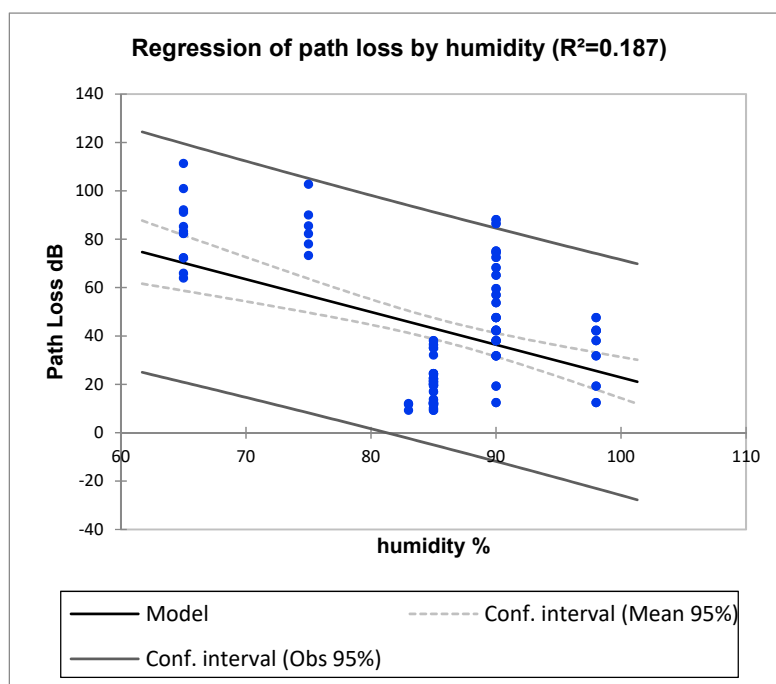


Figure 6. Regression of Path Loss by Humidity.

Based on the linear regression technique on the temperature parameter, Figure 7 shows the regression of the path loss by the temperature with coefficients (0.257). When the temperature increases, the signal strength (RSSI) drops, and if the temperature decreases, the signal strength increases. This outcome specifies a negative relationship between the signal strength and the temperature.

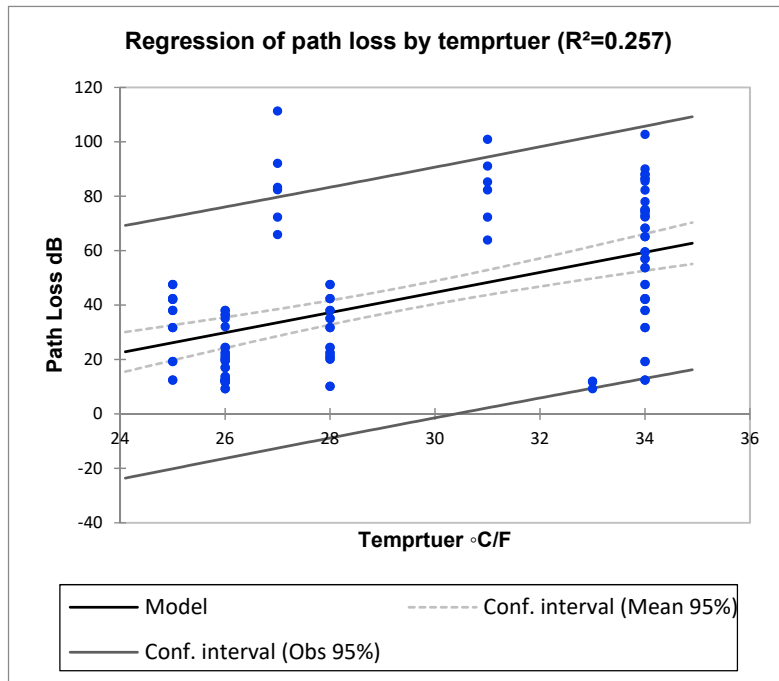


Figure 7. Regression of Path Loss by Temperature.

Based on the linear regression technique on the frequency parameter, Figure 8 shows the regression of the path loss by the frequency with coefficients (0.366). When the frequency increases, the signal strength (RSSI) drops, and when the frequency decreases, the signal strength increases. This outcome specifies a negative relationship between the signal strength and the frequency.

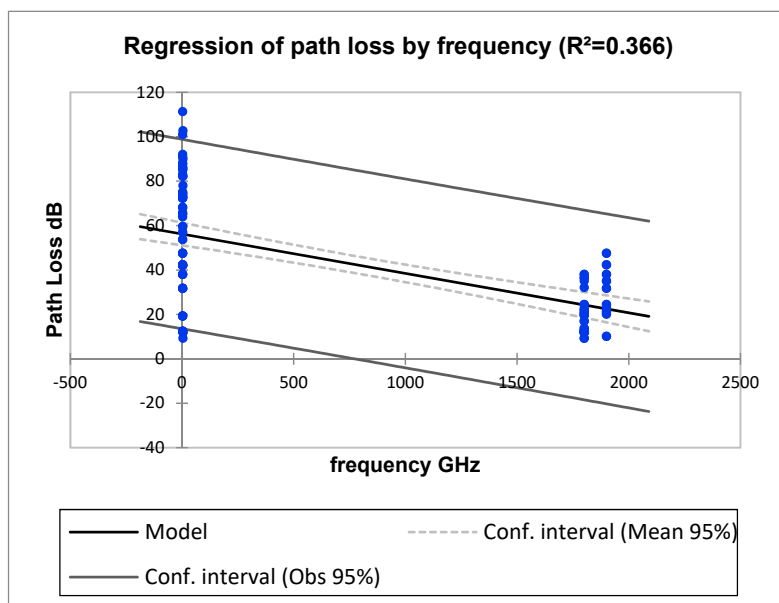


Figure 8. Regression of Path Loss by Frequency.

Figure 9 shows the standard coefficients for all parameters using the linear regression technique and TYM model with a coefficient (96.7).

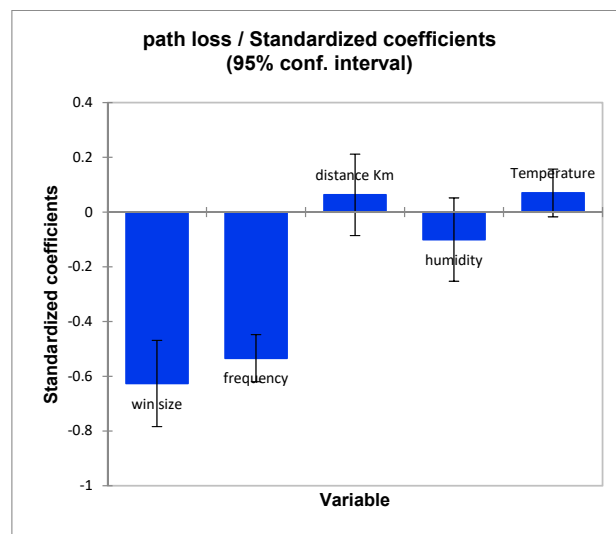


Figure 9. Standardized coefficients (96.7).

4. Results and Discussion

For the analysis of the TYM model, we completed a comparison between the TYM model and two reference models, Okumura and COST 231 HATA, according to the measured data. The expected output results and the measured data in watt was converted into dBm values; the path loss value is given as it is in Equation 8:

$$PL = \text{Transmitted power} + \text{Transmitting gain} + \text{Receiving gain} - \text{Received power} \quad (8)$$

Figure 10 shows the output result from the three reference models: Okumura, COST 231 HATA, and TYM, compared to the measured data. The graph clearly shows that the TYM model has a higher accuracy than the other models, due to its flexibility between high and low frequencies. Meanwhile, the Okumara model only works only with low frequencies. The Okumara model is better than the COST-Hata model, however, because the COST-Hata works exclusively with limited frequencies. Both the Okumara and COST-Hata only focus on outside environments.

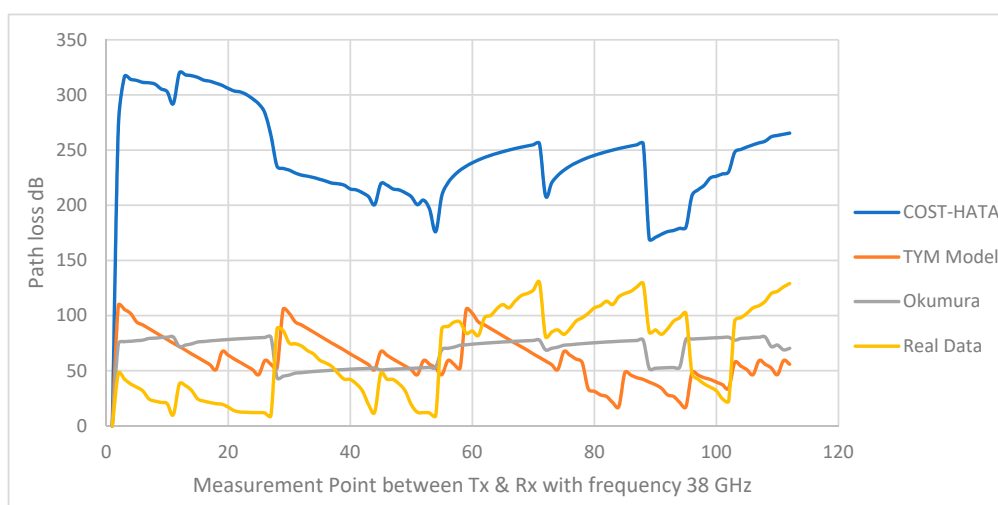


Figure 10. Comparison between the TYM model and the other models with a frequency of 38 GHz.

Figure 11 shows the output result from the three reference models including the real measurement. The Okumura, COST 231 HATA, and TYM models are compared to the measured data. Figures 10 and 11 clearly shows that the TYM model has a higher accuracy than the other models, due to its flexibility between high and low frequencies. Meanwhile, the Okumura model only works only with low frequencies. The Okumura model is better than the COST-Hata model, however, because the COST-Hata works exclusively with limited frequencies. Both the Okumura and COST-Hata models only focus on outside environments, while the TYM model works with outdoor environmental factors such as humidity and temperature in addition to indoor environmental factors such as window size. Additionally, the TYM model worked with 5G, while the Okumura and COST-Hata models did not.

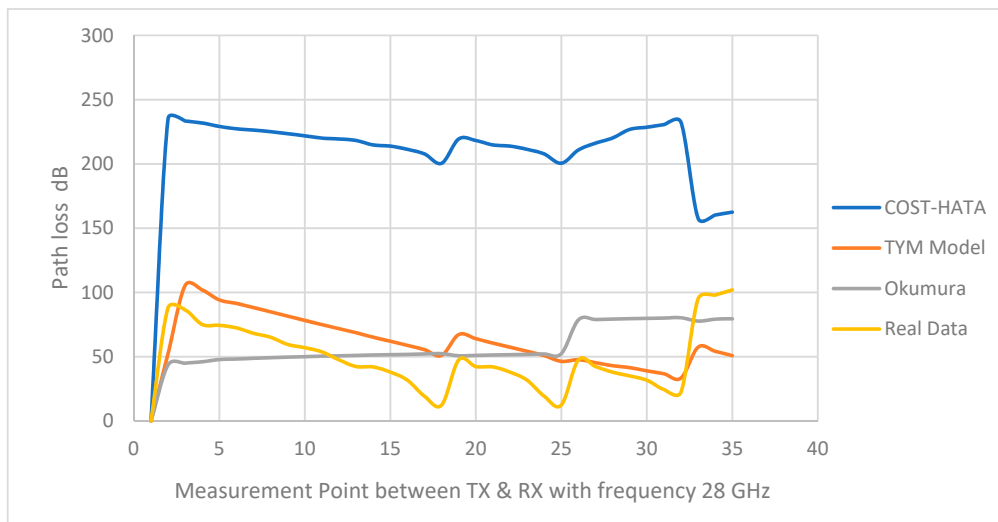


Figure 11. Comparison between the TYM model and the other models with a frequency of 28 GHz.

5. Conclusions

In this paper, we proposed a new path loss model called TYM, which predicted signal strength inside buildings, especially in dead spot areas. The TYM model had new parameters like window size in each floor; weather conditions were also taken into consideration. Moreover, the model 120 total path loss measurements have been included from 35 base stations. We have validated our model over different propagation environments and showed improved results over the Okumura and COST-HATA models. The evaluation analysis proved that the capability of our model over other models compared to real measurements. The TYM model can assist mobile network design engineers to produce stable mobile networks in very accurate and cost-effective ways. Our model enhanced the prediction of path loss by 10% compared to Okumura and by 15% compared to COST-Hata.

Author Contributions: Supervision, N.G. and X.X.; Writing—original draft, Z.N.; Writing—review & editing, N.G., L.A. and X.X.

Funding: This research was funded by the University of Bridgeport, School of Engineering.

Conflicts of Interest: The authors declare no conflicts of interest.

References

1. Popescu, I.; Kanstas, A.; Angelou, E.; Nafornita, L.; Constantinou, P. Applications of generalized RBF-NN for path loss prediction. In Proceedings of the 13th IEEE International Symposium on Personal, Indoor and Mobile Radio Communications, Lisboa, Portugal, 18 September 2002; Volume 1, pp. 484–488.
2. Sulyman, A.I.; Nassar, A.T.; Samimi, M.K.; Maccartney, G.R.; Rappaport, S.T.; Alsanie, A. Radio propagation path loss models for 5G cellular networks in the 28 GHz and 38 GHz millimeter-wave bands. *IEEE Commun. Mag.* **2014**, *52*, 78–86. [[CrossRef](#)]

3. Nossire, Z.; Dichter, J.; Gupta, N.; Fathi, J. A new selected points to enhance radio wave propagation strength outside the coverage area of the mobile towers in the dead spots of cellular mobile WiFi downloads. In Proceedings of the 2015 Long Island Systems, Applications and Technology, Farmingdale, NY, USA, 1 May 2015; pp. 1–7.
4. Alim, M.; Rahman, M.; Hossain, M.; Al-Nahid, A. Analysis of Large-Scale Propagation Models for Mobile Communications in Urban Area. *Int. J. Comput. Sci. Inf. Secur.* **2010**, *7*, 135–139.
5. Alumona, T.L.; Kelvin, N.N. Path Loss Prediction of Wireless Mobile Communication for Urban Areas of Imo State, South-East Region of Nigeria at 910 MHz. *Int. J. Sens. Netw. Data Commun.* **2015**, *4*, 1–4. [[CrossRef](#)]
6. Okumura, Y. Field Strength and Its Variability in VHF and UHF Land-Mobile Radio Service. *Rev. Electr. Commun. Lab.* **1968**, *16*, 825–873.
7. Nadir, Z.; Suwailam, M.; Idrees, M. Pathloss Measurements and Prediction using Statistical Models. In Proceedings of the MIMT 2016, 7th International Conference on Mechanical, Industrial, and Manufacturing Technologies, Cape Town, South Africa, 1–3 February 2016; pp. 1–4.
8. Piazzzi, L.; Bertoni, H.L. Achievable accuracy of sitespecific path loss predictions in residential environments. *IEEE Trans Veh. Technol.* **1999**, *48*, 922–930. [[CrossRef](#)]
9. Wennerstrom, H.; Hermans, F.; Rensfelt, O.; Rohner, C.; Nord'en, L. A Long-Term Study of Correlations between Meteorological Conditions and 802.15.4 Link Performance. In Proceedings of the 2013 IEEE International Conference on Sensing, Communications and Networking (SECON), New Orleans, LA, USA, 24–27 June 2013; pp. 221–229.
10. Zhang, Z.; Sorensen, R.K.; Yun, Z.; Iskander, M.F.; Harvey, J.F. A ray-tracing approach for indoor/outdoor propagation through window structures. *IEEE Trans. Antennas Propag.* **2002**, *50*, 742–748. [[CrossRef](#)]
11. ITU-R P. *Propagation Data and Prediction Methods for the Planning of Short-Range Outdoor Radio Communication Systems and Radio Local Area Networks in the Frequency Range 300 MHz to 100 GHz*; (1411-7); Electronic Publication: Geneva, Switzerland, 2013; pp. 1–41. Available online: <http://www.itu.int/ITU-R/go/patents/en> (accessed on 10 July 2018).
12. Rappaport, T.S.; Sun, S.; Mayzus, R.; Zhao, H.; Azar, Y.; Wang, K.; Wong, G.N.; Schulz, J.K.; Samimi, M.; Gutierrez, F. Millimeter Wave Mobile Communications for 5G Cellular: It Will Work! *IEEE Access* **2013**, *1*, 335–349. [[CrossRef](#)]
13. Hata, M. Empirical Formula for Propagation Loss in Land Mobile Radio Services. *IEEE Trans. Veh. Technol.* **1980**, *29*, 317–325. [[CrossRef](#)]
14. Cavalcanti, B.J.; Cavalcante, G.A.; Mendonça, L.M.D.; Cantanhede, G.M.; de Oliveira, M.M.; D'Assunção, A.G. A hybrid path loss prediction model base on artificial neural networks using empirical models for LTE and LTE-A of 800 MHz and 2600 MHz. *J. Microwaves Optoelectr. Electromagn. Appl.* **2017**, *16*, 708–722. [[CrossRef](#)]
15. Ostlin, E.; Zepernick, H.J.; Suzuki, H. Macrocell radio wave propagation prediction using an artificial neural network. In Proceedings of the Vehicular Technology Conference, VTC2004-Fall, Los Angeles, CA, USA, 26–29 September 2004; Volume 1, pp. 57–61.
16. Murdock, J.N.; Ben-Dor, E.; Qiao, Y.; Tamir, J.I.; Rappaport, T.S. A 38 GHz cellular outage study for an urban outdoor campus environment. In Proceedings of the 2012 IEEE Wireless Communications and Networking Conference (WCNC), Shanghai, China, 1–4 April 2012.
17. Rappaport, T.S.; Gutierrez, F.; Ben-Dor, E.; Murdock, J.N.; Qiao, Y.; Tamir, J.I. Broadband Millimeter-Wave Propagation Measurements and Models Using Adaptive-Beam Antennas for Outdoor Urban Cellular Communications. *IEEE Trans. Antennas Propag.* **2013**, *61*, 1850–1859. [[CrossRef](#)]
18. Nadir, Z.; Elfadhil, N.; Touati, F. Pathloss Determination Using Okumura-Hata Model and Spline Interpolation for Missing Data for Oman. In Proceedings of the World Congress on Engineering, London, UK, 2–4 July 2008.
19. Faruque, S. Propagation prediction based on environment classification and fuzzy logic approximation. In Proceedings of the International Conference on Communications, ICC/SPRINT'96, Dallas, TX, USA, 23–27 June 2002.
20. Miura, Y.; Oda, Y.; Taga, T. Outdoor-to-indoor propagation modelling with the identification of path passing through wall openings. In Proceedings of the 13th IEEE International Symposium on Personal, Indoor and Mobile Radio Communications, Lisboa, Portugal, 18 September 2002.

21. Angeles, C.D.; Dadios, E.P. Neural network-based path loss prediction for digital TV macrocells. In Proceedings of the Humanoid, Nanotechnology, Information Technology, Communication and Control, Environment and Management, Cebu City, Philippines, 9–12 December 2015.
22. EDX Wireless. Smart Planning for Smart Networks. Available online: <http://www.edx.com/> (accessed on 12 January 2012).
23. Hrovat, A.; Kandus, G.; Javornik, T. A Survey of radio propagation modeling for Tunnels. *IEEE Commun. Surv. Tutor.* **2014**, *16*, 658–669. [[CrossRef](#)]
24. Cichon, D.J.; Kurner, T. Digital mobile radio towards future generation systems: Cost 231 final report. In *European Cooperation in the Field of Scientific and Technical Research—Action 231*; Technical Report; European Cooperation in Science and Technology (COST): Brussels, Belgium, 1993.
25. Farhoud, M.; El-Keyi, A.; Sultan, A. Empirical correction of the Okumura-Hata model for the 900 MHz band in Egypt. In Proceedings of the 2013 Third International Conference on Communications and Information Technology (ICCIT), Beirut, Lebanon, 19–21 June 2013; pp. 386–390.
26. Jeng, S.; Chen, J.; Tsung, C.; Lu, Y. Coverage probability analysis of IEEE 802.16 system with smart antenna system over stanford university interim fading channels. *IET Commun.* **2010**, *4*, 91–101. [[CrossRef](#)]
27. Oliveira, J.; Alencar, M.; Rocha, V. A new propagation model for cellular planning. In Proceedings of the IEEE International Telecommunications Symposium, Fortaleza, Ceara, Brazil, 3–6 September 2006.
28. Nossire, Z.; Gupta, N.; Xiong, X. Survey of path loss modeling in wireless communication under various conditions. Unpublished work. 2018.
29. Al-Hamadi, H.M. Long-term electric power load forecasting using fuzzy linear regression technique. In Proceedings of the 2011 IEEE Power Engineering and Automation Conference, Wuhan, China, 8–9 September 2011; pp. 96–99.
30. Tsiropoulou, E.E.; Vamvakas, P.; Katsinis, G.K.; Papavassiliou, S. Combined power and rate allocation in self-optimized multi-service two-tier femtocell networks. *Comput. Commun.* **2015**, *72*, 38–48. [[CrossRef](#)]
31. Saquib, N.; Hossain, E.; Le, L.B.; Kim, D.I. Interference management in OFDMA femtocell networks: Issues and approaches. *IEEE Wirel. Commun.* **2012**, *19*, 86–95. [[CrossRef](#)]
32. Tsiropoulou, E.E.; Katsinis, G.K.; Filios, A.; Papavassiliou, S. *On the Problem of Optimal Cell Selection and Uplink Power Control in Open Access Multi-Service Two-Tier Femtocell Networks*; Springer International Publishing: Cham, Switzerland, 2014.



© 2018 by the authors. Licensee MDPI, Basel, Switzerland. This article is an open access article distributed under the terms and conditions of the Creative Commons Attribution (CC BY) license (<http://creativecommons.org/licenses/by/4.0/>).